Bull. Spec. Astrophys. Obs., 1997, 43, 37-54

Spectral study of MWC 560. Parameters of the system, the hot source and the jets

A.A. Panferov[a], S.N. Fabrika[a], T. Tomov[b]

[a] Special Astrophysical Observatory of the Russian AS, Nizhnij Arkhyz 357147, Russia
[b] National Astronomical Observatory Rozhen, P.O. Box 136, 4700 Smoljan, Bulgaria

Received March 21, 1997; accepted May 12, 1997.

Abstract. Results of spectroscopy of an unusual symbiotic variable star MWC 560 are presented. The data were obtained from autumn 1990 to spring 1993. High velocity absorption lines of H I, D_1 and D_2 of Na I, Fe II(42) and He I are permanently present in the spectra, their radial velocity is $-500 \div -2500$ km/s and changes on a time–scale of a few months. The high velocity absorption line profiles suggest that they originate in a jet, directed closely to the line of sight. These absorptions are variable on a time–scale less than one day and with an amplitude of about 10 %. A fast variability of the absorption line profiles on a time scale of $\lesssim 3$ hours has been detected. Evidence of an opposite (second) jet has been found — there is an additional and variable emission in a red wing of the Hα emission line profile. The radial velocity of this emission corresponds to the jet velocity measured from the absorption lines.

Estimates of the orbital inclination angle ($i \approx 10°$) and the jet parameters have been made. We have simulated the continuous spectrum from UV to IR in the two different states (high and low) of MWC 560. The observed spectrum is formed in a M4–5III giant, a hot source and in an absorbing screen (the jet). The interstellar absorption is $A_V = 1\overset{m}{.}4 \div 1\overset{m}{.}6$. The jet opening angle $2\theta_j \gtrsim 40°$, the jet length in the place of absorption is $\approx 1 \cdot 10^{12}$ cm. The absorbing gas temperature and density are $T_j \approx 8000$ K and $n \approx 5 \cdot 10^{11}\,cm^{-3}$. The jet column density is variable and equal to $N \approx 3 \div 6 \cdot 10^{23}\,cm^{-2}$. In different states of the object only the jet velocity changes (and, accordingly, N), but the mass loss rate in the jet is about constant and equal to $\dot{M}_j \approx 5 \cdot 10^{-7}\,M_\odot$/yr. The object luminosity $L_{bol} \approx 2 \cdot 10^{37}$ erg/s is radiated mainly by the UV source, whose temperature and size are $T \approx 20000$ K and $R \approx 4 \cdot 10^{11}$ cm. The hot source is probably a photosphere of a massive wind ($\dot{M}_j \approx 2 \cdot 10^{-6}\,M_\odot$/yr, $V = 100 - 200$ km/s) rising from the inner area around the white dwarf.

We suppose that both the wind and jets are accelerated in magnetic field of the white dwarf, which accretes the gas from the giant wind as a propeller. The gas flows in accretion disk and is expelled from that by the rotating magnetic field. A sectorial structure of the outflow (jets) is formed. The different states of MWC 560 may correspond to different propeller regimes: a hard propeller with a gas velocity outflow a few thousands of km/s and a soft propeller with a few hundred km/s. The total mass accretion rate onto the propeller is $\dot{M} \approx 3 \div 4 \cdot 10^{-6}\,M_\odot$/yr. The main part of this mass flux (about 50 – 70 %) outflows as a slow wind, $\lesssim 15$ % may reach the white dwarf surface and about 20 – 30 % is expelled as jets. The surface magnetic field strength on the white dwarf is $3 \cdot 10^8\,G \lesssim B_S \lesssim 3 \cdot 10^9\,G$, its rotational period is from 10 – 20 minutes to 3 hours.

Key words: binaries: symbiotic stars: individual (MWC 560) – evolution – jet

1. Introduction

MWC 560 is a symbiotic binary star with an unusual spectrum distinguished by strong variables absorption lines of hydrogen and singly ionized metals. The

© Special Astrophysical Observatory of the Russian AS, 1997

absorption components of the lines in the spectrum of MWC 560 are detached (like BAL quasars) in a sense that there is a portion of undistorted continuum between the absorption and the emission lines. Tomov et al. (1990) have found a shift of these absorptions up to −6000 km/s, which is close to the parabolic velocity of the white dwarf, a likely component in the system. Tomov et al. (1990) have proposed a model of the jet in MWC 560 directed along the line of sight, in which high–velocity absorptions are formed. For the detached absorption components to appear, the radial velocity dispersion in the jet must be considerably lower than the jet spread velocity.

In symbiotic stars jets are known to be observed (Livio, 1996). It is supposed that one of the principal conditions for generation of jets is the presence of an accretion disk (Livio, 1996). A photometric flickering (Tomov et al., 1996) — a typical feature of all cataclysmic variables in which gas accretion by a white dwarf with a magnetic field occurs (Robinson, 1976) — is evidence of the accretion in MWC 560. It is apparent that for the jet gas absorption lines to appear in the spectrum, the gas must be projected onto a continuous spectrum source, that is, the MWC 560 accretion disk axis and therefore the orbital axis of the binary system must be close to the line of sight. The absence of noticeable variations in the radial velocities of the emission lines (Tomov et al., 1994) does suggest such an orientation of the MWC 560 orbit. A host of absorption lines of the jet (of Fe II and other elements with a low excitation potential) form a pseudo-continuum in a UV spectrum. From the modelling of this spectrum Shore et al. (1994) have obtained the column density in the jet to be 10^{23} cm^{-2} for this object being at a maximum UV luminosity (in the spring of 1990) and 10^{24} cm^{-2} at a minimum (in the autumn of 1990).

In this paper we present a spectral monitoring of MWC 560 in 1990–1993 and describe the behaviour of the high-velocity absorption lines, that may be essential for the understanding of their origin. We show that the observed spectrum of the object is formed with involvement of absorption in the jet both in the lines and in the Balmer continuum. Further we model the continuous spectrum with allowance made for the jet absorption and find the parameters of the hot component and the jet.

2. Spectral monitoring of MWC 560. Variability of absorption lines

From October 1990 to February 1993 we obtained about 50 spectra of MWC 560 on the 6 m telescope. The observations were carried out with the spectrograph SP-124 and the IPCS — a TV scanner (Drabek et al., 1986) and with the echelle spectrograph "Zebra" and the panoramic IPCS "Quantum" (Gazhur et al., 1990). A spectral range of 3700–7000 ÅÅ was recorded with a resolution of $\lambda/\triangle\lambda = 3500$ and 2300, an average exposure time for a single spectrum was 20 minutes, and a signal-to-noise ratio was 10–30. The time distribution of the observations allowed us to study a spectral variability from 10 minutes to a week.

In accordance with Tomov et al. (1994) we use the numbering of observing seasons which are determined by visibility of the object for ground-based observations. The first season refers to the first half of 1990, when the absorption lines in the spectrum of MWC 560 showed a maximum velocity and suffered a strong variability from night to night (even disappeared) (Tomov et al., 1990). Our observations refer to seasons 2–4. The dates of the observations and the mean parameters of the high-velocity absorption line Hβ in these seasons — the equivalent width W_λ, the residual intensity I_c, the terminal velocity V_t, determined from the blue wing, the velocity V_c of the centre of mass of the line, and the width at half intensity FWHM — are given in Table 1.

A few typical for these seasons spectra in the region containing Hγ and Hβ lines are shown in Fig. 1. The spectra reduced for a flat field are given in readout IPCS units. It is seen in the figure how the high–velocity absorption lines behave with time.

Strong emission lines of H I and Fe II(42), and deep variable absorption lines of these elements shifted blueward to ≈ -3000 km/s are prominent in the spectrum of MWC 560. Besides those, high–velocity absorptions of D_1 and D_2 Na I, He I and H and K Ca II lines are also present in our spectra, the latter being as deep as the absorptions of H I lines (see also Tomov et al., 1992). In the 3d and 4th seasons broad and very deep H I absorption lines are observed. In the 2nd and at the end of the 4th season the absorption line profiles resemble the P Cyg–type profiles, which appeared as a result of decreasing gas velocity in the jet. The equivalent widths of absorption lines Hα, Hβ and Hγ are approximately equal, which suggests the absorption lines to be saturated, whereas the equivalent widths of the emissions of these lines are an order different from one another. The widths of the emissions are 4–5 times less than those of the absorptions. The observed profiles, for instance, of the Hγ line are unlike those calculated for a spherically symmetric outflow (e.g. see Castor and Lamers,

Table 1: *Parameters of* Hβ *absorption in 1990–1993*

season $\mathcal{N}$	date of observations	I_c	W_λ Å	V_t km/s	V_c km/s	FWHM km/s
2	9.10.90 – 15.10.90	0.1	8 ÷ 11	900 ÷ 1400	400 ÷ 500	500 ÷ 700
	15.04.91	0.2	4.1	580	190	320
3	29.10.91 – 21.3.92	0.1	15	2500 ÷ 2800	1700 ÷ 1900	1000
4	21.09.92 – 10.12.92	0.1	15 ÷ 20	2500 ÷ 2900	1600 ÷ 1900	1000 ÷ 1300
	9 – 10.02.93	0.1	9 ÷ 12	1700 ÷ 1900	1200	600 ÷ 800

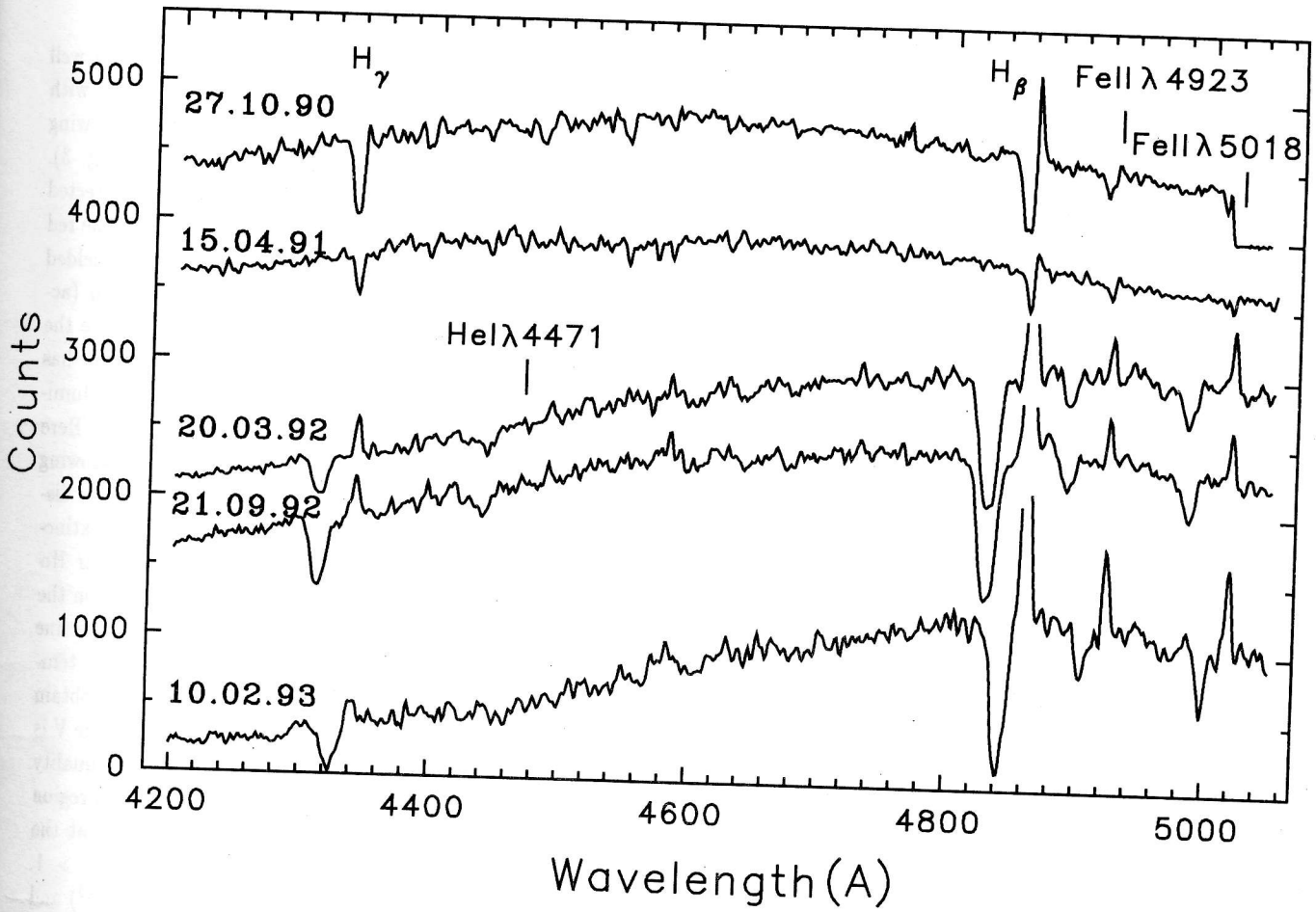

Figure 1: *Spectra of MWC 560 within 4200–5040 Å, obtained at different seasons. The dates of observations are shown. Counts are indicated on the vertical axis. From top to bottom the spectra are shifted in intensity by 4000, 3400, 2000 and 1300 units. Emission of* Hβ *line is cut on three lower spectra.*

1979). The equivalent width ratio of the Hγ absorption and emission lines is smaller than 0.1, which requires the optical thickness $\tau < 1$ for the spherical wind (Castor and Lamers, 1979), nevertheless from the great absorption line depth it can be concluded that $\tau > 1$. The observed absorption lines do not resemble the absorptions formed in the anisotropic wind either as, for example, in the cataclysmic variable RW Sex, in which the wind velocity amounts to 4300 km/s (Greenstein and Oke, 1982). So, the high–velocity absorption lines in the spectrum of MWC 560 may be formed in the jet directed to the observer.

In Fig. 2 are shown the absorption line profiles of different elements, which have been obtained from the echelle spectrum of December 9, 1992. It is seen that the widths of the Fe II absorption lines are smaller than those of the H I absorption lines. The absorption lines Fe II λ 4924 and λ 5018 may be blended with the

absorption lines He I λ 4922 and λ 5015, respectively. The latter, however, are much weaker than the lines of iron since the intensities of other He I absorption lines are small. It can be seen from Fig. 2 that the jet is inhomogeneous in both velocity and temperature.

The intensities I_c of the absorption lines H I are the same for different seasons, but for the end of the 2nd season. The decrease in I_c and FWHM of the absorption lines in the spring of 1991 (Table 1) is due to the fact that the absorption lines approach the emission lines. High excitation lines typical of symbiotic variables have not been revealed in our spectra.

The time resolution in the study of variability from our spectra on different dates was from 10 minutes to 5 hours. The quality of spectra on some dates was sufficient for 3 % of variability to be detected. A daily variability of high-velocity absorptions with an amplitude of 10–20 % was always observed, which is seen from Fig. 3, where the behaviour of the Hγ, Hβ and Hα absorption lines from the spectra taken from December 4 to 10, 1992 is shown.

To demonstrate the variability, we show the differences between the spectra under study and a reference spectrum, which is a sum spectrum over all the observations (at the top in Fig. 3). However the fragment of the reference spectrum with the Hα line is presented from the spectrum on December 9 to show more vividly the broad red wing of this line (manifestation of the counter jet, see below). All the spectra have been reduced to residual intensities. The vertical dashed lines indicate a zero radial velocity and -2800 km/s (± 2800 for the Hα). The profile variability of the high-velocity absorptions can be seen in all the spectra in the lines Hα, Hβ and Hγ. The variability of the absorptions in the spectra on December 8, which were obtained with an interval of 3 hours, can also be seen in the figure: the change in the intensity occurred simultaneously for the absorption lines Hγ and Hβ at $V_r = -2360$ and -1090 km/s. At the same time no changes in Hα absorption were noticed, possibly because of the great optical thickness of this line. In the examples of the night-to-night variability, Hα is markedly different from the lines Hγ and Hβ, whose absorption line profile variability is practically synchronous. The amplitude of the 3-hour's variability in Hγ and Hβ is not smaller than that of the night-to-night variability. In spite of the fact that occasionally the variability amplitude slightly exceeds the noise in the spectra the apparent synchronism of the variations in the Hγ and Hβ absorption line profiles makes this variability significant. On other nights no fast variability was noticed, that is why the differences for the night's sum spectra are only presented for these nights. A variability of high–velocity absorptions in the UV spectra at times of $\lesssim 3$ hours has been detected by Michalitsianos et al. (1991), while at times of about 1 hour — by Fabrika et al. (1991). Based on this variability we can estimate the jet length. Taking the characteristic time of the variability $\Delta t \lesssim 3$ hours and the gas velocity in the jet during the observations on December 1992 $V_j \approx 2000$ km/s we find $R_j \leq \Delta t \cdot V_j \approx 2 \cdot 10^{12}$ cm.

A broad red wing in the Hα emission line is well visible on the spectra; its width is comparable with the width of the absorption line (Fig. 2). The wing also shows variability from night to night (Fig. 3). We suppose that the radiation of the jet directed away from us (the counter jet) contributes to the red wing of the Hα line. This radiation may be shielded partially by the hot component of the system (accretion disk). The excess in the red wing above the Hα line core profile approximated by Gaussian has an equivalent width of about 4 Å. The total luminosity in this wing is $L(H\alpha) \gtrsim 2 \cdot 10^{33}$ erg/s. Here we have adopted the mean values of the following parameters (see Table 2 and Fig. 5 below): the distance to MWC 560 — 1.7 kpc, the interstellar extinction and the flux in continuous spectrum near Hα — about 1^m and $F_\lambda = 5 \cdot 10^{-13}$ erg/cm^2 s Å. On the basis of the specific emission measure in the Hα line $\approx 2 \cdot 10^{-26} N_e^2$ erg/s cm^3 ster, for the expected temperature in the jets $\approx 10^4$ K (see Table 2) we obtain the emission measure: $V n_e^2 \gtrsim 6 \cdot 10^{57}$ cm^3, where V is volume, n_e is the electron density. Here the inequality conforms to the fact that part of the emission region is screened by the accretion disk and also that the optical thickness of the emitting gas may be > 1. Assuming that the jet is conical ($V \approx \sin^2 \theta_j R_j^3$) and using the jet length obtained from the time of variability, we can estimate the column electron density in the jet $N_e = n_e R_j$. Assuming that the semi–opening of the jet in MWC 560 is $\theta_j = 20°$, we obtain $N_e \gtrsim 1.6 \cdot 10^{23}$ cm^{-2}. Below based on the modelling of the continuous spectrum of MWC 560 we determine the total column density (the number of protons + the number of hydrogen atoms) of the absorbing gas in the jet, $N_H \approx 10^{24}$ cm^{-2}. This has been derived for the jet directed toward us while the electron density N_e has been found from observations of the counter jet. We have not any grounds to believe that the two jets differ in their properties, therefore it follows from these two values that the hydrogen ioniza-

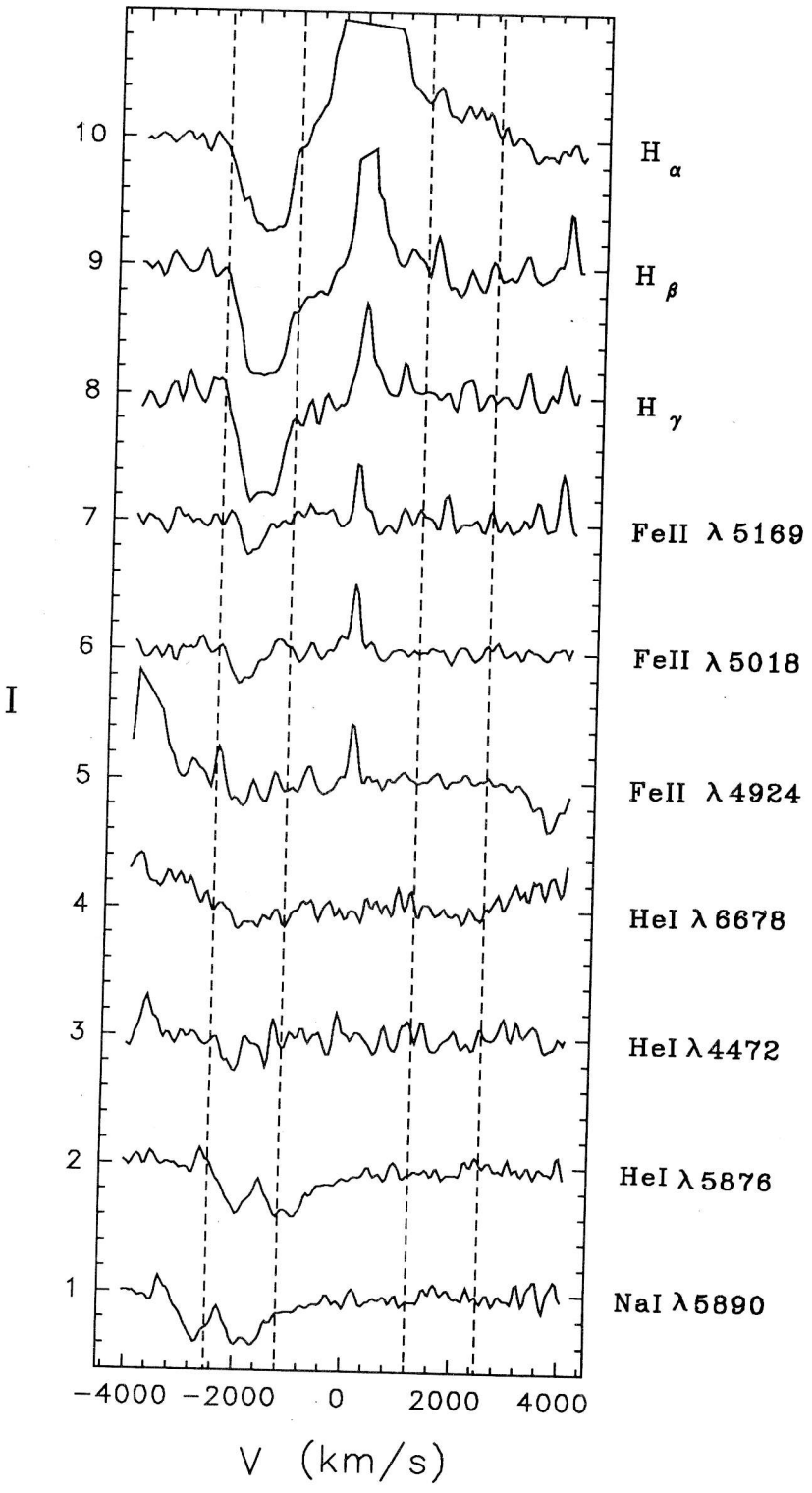

Figure 2: *Profiles of high–velocity absorptions, obtained on December 9, 1992 (UT = 9.931). Horizontal axis shows the velocities with respect to the laboratory wavelength, the vertical – residual intensities. The dashed lines are given for a convenience of comparing these profiles.* Hβ *and* Hα *emissions are cut.*

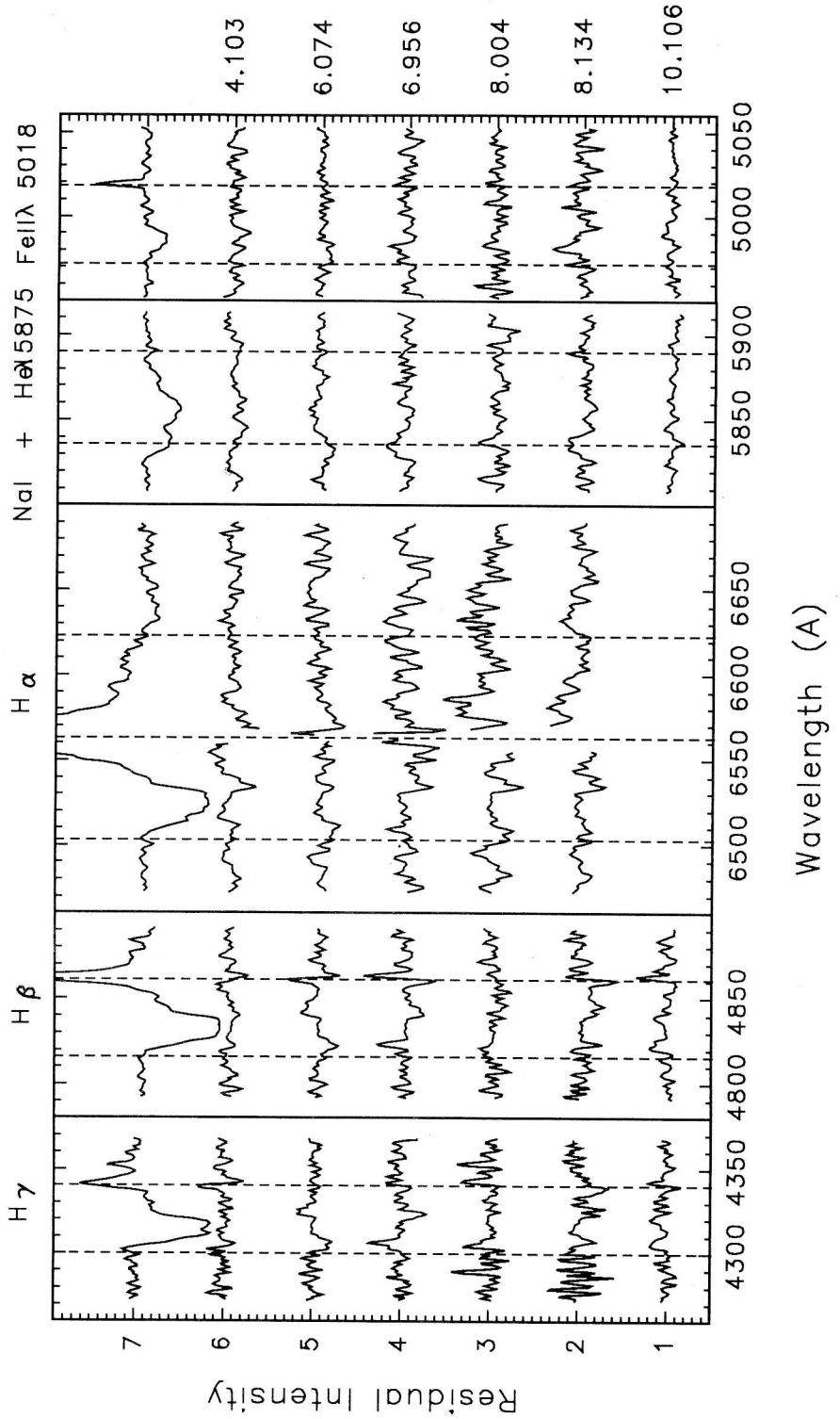

Figure 3: *The summary line profiles of* $H\gamma$, $H\beta$, $H\alpha$, D_1, D_2 Na I + He I λ 5875, Fe II λ 5018 *and their differences with those of December 4–10, 1992. All the spectra are normalized. A daily variability is noticed. The spectra on December 8 show absorption variability for 3 hours. The time of observations (UT) is indicated right. The vertical dashed lines are given for a convenience of the profiles comparing.*

tion degree in the MWC560 jets $n_e/n_H \gtrsim 0.15$, i. e. the gas temperature $T_j \approx 7000 \div 10000$ K. Note that this estimate of the ionization degree in the jets does not depend on the volume filling factor of the gas, i. e. on whether the gas is in clouds or the whole volume of the jet is completely filled with the gas.

The results of observations are in good agreement with the idea that the MWC560 jets are oriented close to the line of sight. It is natural to suppose that the jets are perpendicular to the accretion disk, i. e. the axis of the jets is parallel to the angular momentum of accreted matter. From this it also follows that the orbital inclination angle is small. From the data of Tomov and Kolev (1997) the radial velocity of the Fe II, Ti II and of other metal emission lines is about 35 km/s and does not change in time; within an interval of more than 1000 days the radial velocities change by less than 4 km/s. On the basis of CCD spectra taken later on the 6 m telescope E. L. Chentsov (private communication, 1997) has reported the amplitude of radial velocity variations of the emission lines to change by less than 2 km/s, here again for a time of more than 1000 days. The metal emission lines are produced as a result of fluorescence of UV radiation (Shore et al., 1994) and, apparently, belong to gas outflowing from the inner regions. Thus, we can estimate the upper limit to the amplitude of orbital variability of radial velocities as $2K \lesssim 4$ km/s. The orbital period of MWC560 determined by Doroshenko et al. (1993) from the data of archives and up-to-date photometry is 1930 days. Assuming the masses of the white dwarf and the giant to be $1M_\odot$ (see the discussion below), we find the orbital velocity $V_{orb} \approx 10$ km/s and the restriction on the possible interval of the system's inclination angle value $\Delta i \leq K/V_{orb} \cos i \approx 10°$. The probability of finding a binary system with $i = 0°$ is extremely low, therefore we may take $i \approx 10°$ for the inclination angle of the system.

From modelling the continuous spectrum of MWC560 (Table 2) we estimate the size of the UV radiation source of about $(4 \div 5) \cdot 10^{11}$ cm. For the observed absorption lines to appear in the jet, the size of the jet projection onto the sky plane (in the jet where the absorbent is situated, $R_j \lesssim 2 \cdot 10^{12}$ cm) must be larger than that of the source. From this condition it follows that $\theta_j - i > 10°$. Taking into account the inclination angle of the system (and the jet), $i \approx 10°$, we find that the semi-opening of the jet is $\theta_j \gtrsim 20°$. In the known symbiotic binary CH Cyg this parameter determined from radio observations (Taylor et al., 1986) is $\theta_j \approx 5°$.

The MWC560 jet opening angle can also be estimated based upon the jet absorption line widths of detached P Cyg type. This will be an upper limit to the value since along with the dispersion of trajectories of matter in the jet there are other mechanisms (e. g. the dispersion of gas ejection velocities) that may contribute to the absorption lines broadening. The jet is inhomogeneous in both temperature and density. This follows from the variability of the high-velocity absorption lines and from the fact that we observe absorptions of elements of essentially different excitation potentials (Fe II, He I). Collision of individual fragments of the jet at velocities of several hundred km/s must cause considerable temperature variations of the jet gas. From examples of detached P Cyg profiles on the spectra of different dates in early 1990 (Tomov and Kolev, 1997) we find that the ratio of the minimal width of the observed absorption lines to the maximal velocity of ejection on the same dates is equal to $FWZM/V_t \approx 0.2$. So we have from this $\theta_j - i < 35°$ or $\theta_j < 45°$. Here the inequality conforms to the fact that the absorption line broadening is caused not only by the dispersion of trajectories of the gas motion but also by the dispersion of gas velocities in the jet.

3. Dependence of MWC 560 brightness on the jet velocity

The spectrum of MWC560 is formed in the M4–M5 giant star and the hot source of spectral class B5–A0 (Zhekov et al., 1996). IR radiation has been noticed to be slightly variable on time scale of a few days, which is typical of late giants, although the mean brightness has not changed for several years (Zhekov et al., 1996). At the same time the optical brightness, especially the UV, is subject to both rapid variability (flickering) and more considerable long-time variations (Tomov et al., 1996). Zhekov et al. (1996) have found that the colours of the hot component do not agree with those expected from the accretion disk. However they disregarded a possible absorption by matter of the jet. At the column density of hydrogen in the jet $N_H = 10^{23 \div 24}$ cm^{-2} (Shore et al., 1994) this absorption must be essential in formation of the observed spectrum in the UV and even in optics. Therefore, the variable mass flux in the jet (or even the variable gas velocity in the jet at a constant mass flux) may be the cause of the radiation flux variability.

In Fig. 4 are shown the time dependences of the

velocity V_c and radiation fluxes of the object in the V band (Tomov et al., 1996) and in the UV. A correlation is well seen in the velocity variations of the gas ejection and the UV flux. The flux from the object in optics also shows similar variations, however the amplitude of the flux variations in the V band is small, and the relation between the two quantities may be more complicated.

By the fall of 1990, in the 2nd observing season the mean outflow velocity in the jet dropped to $V_c \approx 500$ km/s and became even lower in the spring of 1991 ($V_c \approx 200$ km/s). This was accompanied by a decrease in brightness to $0^m.5$ and by the reddening $\triangle(U-B) \approx 0^m.5$ and a more dramatic fall in UV radiation intensity (compared to the spring of 1990). In the 3d season by the autumn of 1991 the velocity increased and kept increasing till 1992. In 1992 the V band luminosity was growing as well. Between 1992 and 1993 the velocity was observed to decrease a little at the constant brightness of the star. Further the velocity did not change much. In the period under study the object MWC 560 was in a passive state, when the absorption lines had a minor variability as distinct from the very active state in the spring of 1990, when the absorption lines were observed to be strongly variable (Tomov et al., 1990). The brightness variations in the passive state are also smaller than in the active one.

In the 2nd season in the spring of 1991 the velocity of the jet was by approximately a factor of 5 lower than the mean velocity in the periods that followed and by an order lower than the velocity in the 1st season. The cardinal changes in the UV spectrum took place too (Fig. 4). The total UV intensity in the 2nd season was lower, than both in the 1st and in subsequent seasons, about 5–6 times as small, while in the range shorter than 1400 Å the difference was still greater (Maran et al., 1991) and amounted to several dozen times. The UV spectrum in September 1990, when the velocity of gas in the jet dropped to ≈ 1000 km/s, was similar to those of classical novae several days after the maxima. This type of spectra has been called "the iron curtain" (Shore et al., 1994): powerful unidentifiable emission features, which, in fact, are the portions of the continuum that remained after absorption of the strong UV multiplets of Fe II and other ions of low ionization potentials in moving matter. Such dramatic changes in the UV were practically not reflected in the optical range, where these ions do not absorb. The strong variations in the UV were thus caused by the variations of the optical thickness of the absorbing gas, the real UV source luminosity was likely to be unchanged. Since the redistribution of energy has not been observed, then this gas is optically thick only in the directions close to the line of sight, which is consistent with the jet outflow model. The variation of column density of absorbing gas between different states of UV brightness (Shore et al., 1994) reflects the gas mass variation on the line of sight within the zone of ionization of principal absorbing agents. We suppose that the decrease in velocity of gas observed in the 2nd season caused the increase in N_H. Thus, physical conditions in the jet affect the shape of the UV spectrum of MWC 560. This will be shown by the spectrum modelling.

4. Modelling the continuous spectrum of MWC 560

From the absorption lines of Ti O Thakar and Wing (1992) have defined the spectral type of the giant in MWC 560 as M4–M5. When modelling, we have used colours and absolute magnitudes of giants M4 and M5 from the data of Lang (1992). Optical and UV spectra of symbiotic stars are peculiar, and for their explanation 4 models of a hot radiation source are usually used: 1) a hot star in a planetary nebula, 2) a hot surface of a white dwarf, at which permanent nuclear burning of accreted matter occurs, 3) an accretion disk, 4) a hot optically thick wind from a white dwarf. Models 1 and 2 are inconsistent with the fact that high excitation lines are not observed in the spectrum and with the high luminosity of the object (Table 2). Models 3 and 4 are likely to be more suitable for the description of MWC 560. The observed flickering may be evidence of gas accretion onto a star with a magnetic field (Robinson, 1976). The accretor in MWC 560 is, apparently, a white dwarf since the maximal observed velocity of the gas outflow (6000 km/s) is close to the parabolic velocity of a white dwarf.

The observed luminosity of MWC 560 is an order lower than critical Eddington luminosity. This suggests that the supercritical accretion disk can not be considered as the source of the jets. In the case of model 4 the wind may be due to thermonuclear bursts of matter accumulated at the white dwarf surface in the process of accretion or a rotating magnetic field of the white dwarf acting like a propeller (Illarionov and Sunyaev, 1975). We have considered models 3 and 4 for the hot component as an accretion disk in geometrically thin and locally blackbody approximations (Shakura and Sunyaev, 1973) with a boundary layer (Lynden-Bell and Pringle, 1974) and as a sphere with

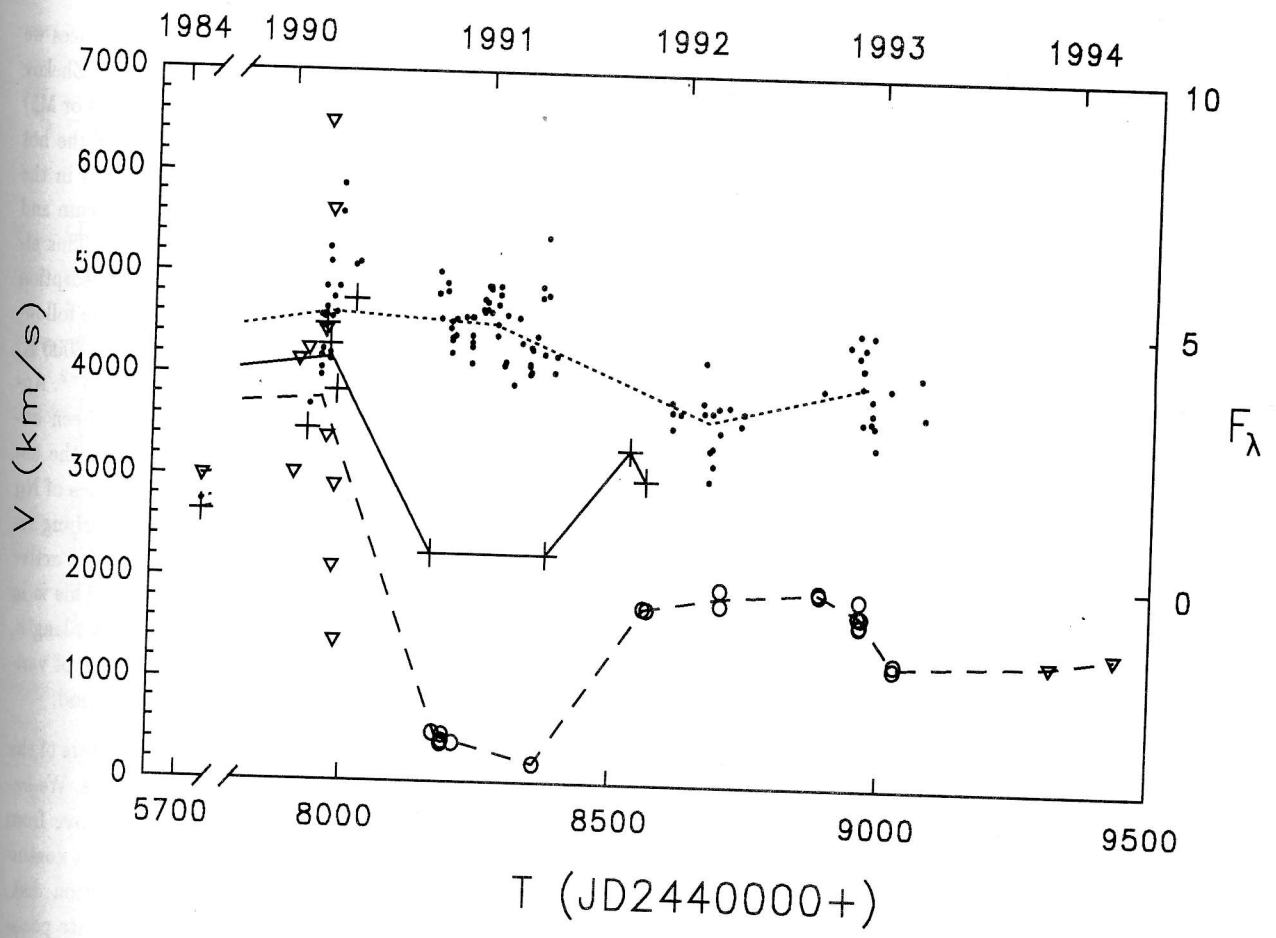

Figure 4: Time variations of MWC 560 activity. The Hβ line centre of mass velocity V_c is shown (circles — our data, triangles — Tomov et al. (1990; 1992; 1994)). Radiation fluxes in optics — dots, in UV — crosses. The axes show: left — the velocity in km/s, right — the radiation flux in 10^{-13} erg cm^{-2} s^{-1} Å^{-1}. Bottom — the time in days (JD 2440000+), top — in years.

blackbody radiation. The jet has been modelled as a homogeneous hydrogen layer in an LTE state, which absorbs radiation from the hot source. The velocity of gas motion was assumed equal to 1000 km/s. This velocity does not affect the shape of the continuum, but only slightly changes the position of the Balmer jump. For the assumed temperatures of gas in the jet of MWC 560 (5000–10000 K, see above and also Shore et al., 1994) the following basic processes of absorption and scatter of continuous radiation have been taken into account: free-bound and free-free transitions of atoms and negative hydrogen ions, Rayleigh scattering by hydrogen atoms and Thomson scattering by free electrons. The model spectrum of continuous radiation has been obtained with allowance for interstellar extinction for which the approximations of Cardelli et al. (1989), O'Donnell (1994) and the value $R_V = A_V/E_{(B-V)} = 3.14$ have been used.

The model spectrum was compared with the observed spectrum which has been obtained from the UBV data of Tomov et al. (1996), JHK data of Zhekov et al. (1996) (see references therein) and UV data of IUE observations of Michalitsianos et al. (1991) and Fabrika et al. (1991). From the UV data the fluxes near λ 1470 and 3100 Å have been only used, where the continuum radiation is clearly seen between the strong absorption bands. We have chosen two UV flux states of MWC 560 (and corresponding to them the optical fluxes, see Fig. 4): with the maximal flux — in the spring of 1990 (Michalitsianos et al., 1991) and with the flux typical for the main, more quiet, state of the object (Fabrika et al., 1991) — in the autumn of 1991. These two states correspond to the active and passive periods (Table 1) determined above on the basis of gas outflow velocities and brightness of the object. They are also different in variability of the star: in the active state the object is more variable. From examination of Fig. 4 and analyzing the mov-

ing absorption line profiles in different seasons (e.g. Tomov and Kolev, 1997) it can be concluded that MWC 560 actually exhibits a whole set of states. The transitions from one state to another may be rapid (it can be only said about the transition time that it is shorter than a few months), but the characteristics of the object (velocity in the jets, UV and optical brightness and variability amplitude) change from a state to state continuously. So it could be more correctly to say about the object activity levels in different observational seasons than about the active or the passive states. Nevertheless, for modelling the spectrum we have chosen two seasons corresponding to the two states of the object, hereafter passive and active.

In Table 2 are listed the parameters of the system derived from the models. Designations of the models: ad — an accretion disk, bb — a sphere with blackbody radiation, 1 — active state, 2 — passive state, M4 III and M5 III — spectral class of the giant star in the given model. Parameters of the models: D — the distance to the system, $A_V(G)$ and $A_V(H)$ — interstellar extinction in the V band determined from the spectra of the giant and the hot component, respectively, R_{in} — the inner radius of the accretion disk, R_{out} — the outer radius of the disk or radius of the sphere, T — the temperature of accretion disk on radius of $2.25\,R_{in}$ (where maximum contribution to the total luminosity is (Shakura and Sunyaev, 1973)) or the temperature of the sphere, $\dot{M}_a$ — gas accretion rate, L_{bol} — the bolometric luminosity of the hot component. T_j, N_H, n — the temperature, column and volume densities (hydrogen and protons) of absorbing gas in the jet. For the models with an accretion disk we have used $1\,M_\odot$ as the white dwarf mass value, which is the average white dwarf' mass in cataclysmic variables (Ritter, 1991).

In Fig. 5 are shown the data of observations and the simulated spectra in the models bb1 + M5 III (solid line) and bb2 + M5 III (dashed line) for the active and passive states, respectively. The vertical bars show uncertainties in the observational data. The large scatter in the radiation fluxes in the optical and UV ranges of the spectra in the active state corresponds to the actually observed variability of the object. The models are consistent with the observations. The other models from Table 2 fit the observational data as well. The discrepancies of the models χ^2 are given in Table 2.

In our models the distance to the system is determined by the luminosity of the giant star. However, this procedure is burdened with uncertainty in absolute stellar magnitude of the giant. The distances we obtained are in agreement with the results of Zhekov et al. (1996). The choice of the giant type (M4 or M5) has no essential effect on the parameters of the hot component. The parameters of absorbing gas in the jet affect basically the shape of the UV spectrum and the spectrum break near the Balmer jump. This allows us to separate two effects: the jet gas absorption and interstellar extinction. We have found the following parameters of gas in the jet: $T \approx 7000 \div 8000$ K, $n \approx 5 \cdot 10^{11}$ cm^{-3}, $N_H \approx 3 \cdot 10^{23} \div 1 \cdot 10^{24}$ cm^{-2}. Approximately the same values for N_H have been obtained by Shore et al. (1994) by modelling the absorption UV spectrum. From the found values of N_H and n we derive the jet length (of the absorbing region in the jet) to be $3 \div 6 \cdot 10^{11}$ cm in the active period and $1 \div 2 \cdot 10^{12}$ cm in the passive. This is in good agreement with the constraint on the jet length, $R_j \lesssim 2 \cdot 10^{12}$ cm, found above from the time of variability of absorption lines in the passive period.

In both models (ad and bb) the parameters of the hot source and jet turn out to be quite close. We believe that the two models are not alternative from the point of view of description of the object continuous spectrum. The presence of the accretion disk, at least its outer region, in MWC 560 is quite possible. The central region around the white dwarf may be screened from the observer by an optically thick expanding wind, whose photosphere is the UV radiation source. The model bb is more self-consistent (see below). It can be concluded from Table 2 that in both states the rate of mass loss is the same. N_H in the active state is a few times less than in the passive one, in the bb model this factor is 2. The gas velocity in the jet in the passive state (the autumn of 1991) is about twice as low as in the active. Since the mass loss rate is $\dot{M}_j \propto N_H V_j$, both states do not differ in $\dot{M}_j$ (unless the jet opening angle changes in the different states). We have assumed above that all basic properties of spectrum variations can be explained only by the variable jet velocity. The assumption has been confirmed by the results of spectrum modelling.

When simulating the accretion disk spectrum we took into account only the part of the disk that had a temperature higher than 10000 K. At lower temperatures hydrogen is ionized only partially and gas cooling in lines becomes essential, which causes overestimation of the continuum level in the model. In the accretion disk model the UV spectrum depends on R_{in}, $A_V(H)$ and the jet parameters most of all. It appears that a fitted value of R_{in} is close to the

Table 2: Models

Parameters	ad1		bb1		ad2		bb2	
	M4 III	M5 III	M4 III	M5 III	M4 III	M5 III	M4 III	M5 III
D [kpc]	1.43	2.00	1.43	2.00	1.42	2.00	1.42	2.00
A_V(G)	1.64	1.10	1.62	1.10	1.61	1.03	1.57	1.10
A_V(H)	1.26	1.17	1.46	1.44	1.27	1.12	1.29	1.57
R_{in} [10^{10} cm]	4.4	7.3	—	—	4.3	7.8	—	—
R_{out} [10^{10} cm]	48.7	67.7	38.6	54.1	41.5	58.7	36.3	54.8
T [10^4 K]	2.72	2.40	2.11	2.08	2.50	2.10	1.79	1.99
$\dot{M}_a$ [10^{-5} $M_\odot$/y]	9	25	—	—	6	18	—	—
L_{bol} [10^{37} erg/s]	1.73	2.90	2.10	3.90	1.18	1.95	0.96	3.35
T_j [10^4 K]	0.78	0.78	0.78	0.78	0.68	0.68	0.78	0.78
N_H [10^{23} cm^{-2}]	2	2.5	3	3	10	12	6	6
n [10^{11} cm^{-3}]	6	5	5	5	6	6	5	5
χ^2	0.39	0.39	0.34	0.38	0.78	0.49	0.47	1.03

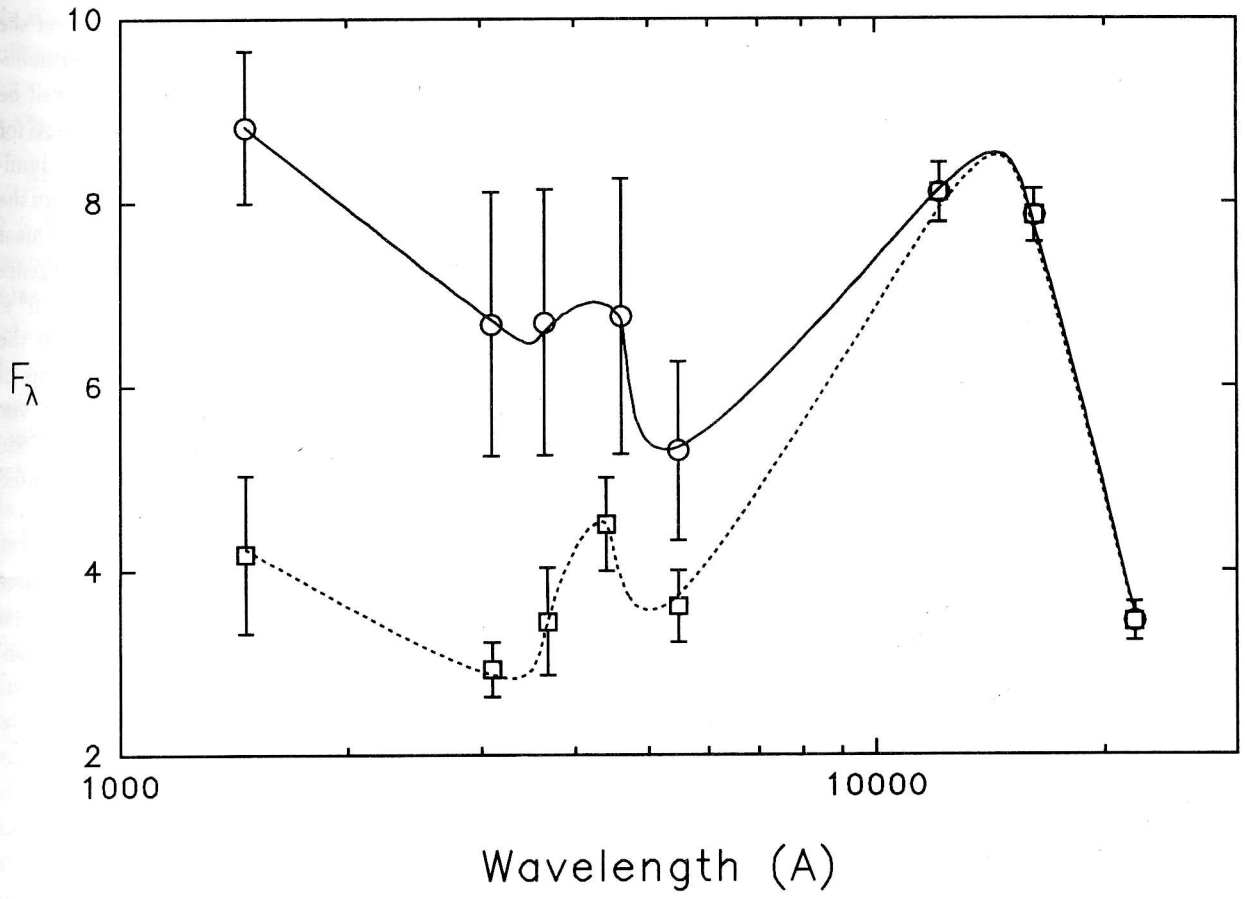

Figure 5: The continuum spectrum of MWC 560. Circles and squares — the data of observations in the active and passive states of the object. Solid and dashed lines — the spectra of models: bb1 (M5 III) and bb2 (M5 III). The wavelengths are in logarithmic scale. Intensity is in 10^{-13} erg cm^{-2} s^{-1}.

radius of normal stars. Decrease in R_{in} causes increase in bolometric luminosity and N_H, in particular for $R_{in} = 5 \cdot 10^8$ cm (the radius of the white dwarf of mass $1M_\odot$) we have $L_{bol} > 10^{39}$ erg/s and $N_H \approx 5 \cdot 10^{24}$ cm^{-2}, and the most of the luminosity being in the hard UV range. The best fit of the model spectrum to the observed is achieved at $R_{in} \approx 4 \div 8 \cdot 10^{10}$ cm. The accretion rate is determined unambiguously from the optical spectrum and turns out $\sim 10^{-4} M_\odot$/yr; in the active state it is higher than in the passive by about a factor of 1.5. The bolometric luminosity of such a truncated accretion disk equals $1 \div 3 \cdot 10^{37}$ erg/s.

The accretion disk model describes fairly the observed spectrum, but, nevertheless, it is not suited to the system MWC 560 since it requires an impossibly high accretion rate and a large inner radius of the disk. The necessary accretion rate is $\sim 10^{-4} M_\odot$/yr. Besides that, it is unclear how the matter from the outer region of the disk is utilized. If this matter outflows, then, in fact, this is the case of the bb-type model, in which the required gas accretion rate is by two orders lower. The principal problem for all the models — the great UV luminosity of the source and the relatively low accretion rate ($\sim 10^{-6} M_\odot$/yr), which may be provided by the red giant — can be naturally resolved in the bb model. We will discuss therefore only this model of the hot source — the blackbody radiating sphere.

The two considered spectral types of the giant star, M4 and M5, yield quite close parameters of the source and jet. Nevertheless, it can be seen from Table 2 that the value of interstellar extinction determined from the M5 giant spectrum is systematically lower than that found from the spectrum of the UV source. The cool envelope of the giant may well contain a dust, therefore it would be naturally expected that $A_V(H) \leq A_V(G)$. This is the case for the model with M4 giant, so we consider it more preferable. The most likely parameters of MWC 560 derived from the models bb1 and bb2 + M4 giant are the following: the distance to the system D = 1.4 kpc, the light extinction $A_V(H) \approx 1^m.4$ and $A_V(G) \approx 1^m.6$, the UV source temperature ≈ 20000 K, its radius $\approx 4 \cdot 10^{11}$ cm, its luminosity is $2 \cdot 10^{37}$ erg/s in the active state and $1 \cdot 10^{37}$ erg/s in the passive state, the jet gas temperature ≈ 7800 K, its density on the line of sight is $3 \cdot 10^{23}$ cm^{-2} in the active state and $6 \cdot 10^{23}$ cm^{-2} in the passive state.

The photosphere of an optically thick wind conforms to the blackbody sphere model considered. This photosphere absorbs all direct photons from the white dwarf surface or from the inner regions, e. g. from the magnetosphere. This may also account for the absence of hard UV radiation and high excitation absorption lines in the spectra of MWC 560. Such a wind may arise 1) when the accretion luminosity exceeds the critical value, 2) as a result of thermonuclear burning or bursts at the surface of the white dwarf (Paczynski and Zytkov, 1978), and 3) as a result of propeller mechanism action. The bolometric luminosity of MWC 560 is by an order lower than the critical corresponding to electron scattering. If the hard radiation affects the unionized gas above the accretion disk, the critical luminosity needed for gas acceleration, may be markedly lower. Such a model requires an axially-symmetric cocoon to be created above the internal parts of the accretion disk, which, by itself, suggests the presence of other mechnisms for destruction of the disk and gas acceleration. In continuous thermonuclear burning of matter accreted onto the surface of the degenerate star, to ensure the observed luminosity $\sim 10^{-(6 \div 7)} M_\odot$/yr is needed, however the mechanism of gas ejection is absent. With thermonuclear bursts the luminosity in a burst may well be higher than the Eddington luminosity necessary for outward acceleration of gas. For the dramatic luminosity variations in the bursts to be obscured from the observer, the time intervals between the bursts must be much shorter than the time of radiation emergence from under the photosphere, i.e. $\ll R_{out}/V_j \sim 10^3$ s. However the intervals between the bursts with the accretion rates being discussed amount to dozens of years (Paczynski and Zytkov, 1978), therefore the thermonuclear model of gas acceleration in MWC 560 is not suitable. We suggest that matter is accelerated by the propeller mechanism.

In a number of papers devoted to investigation of MWC 560 (e.g. Tomov et al., 1994) it is assumed that in the passive state the white dwarf accretes gas under the propeller condition, while in the active state (e. g. in periastron the rate of accretion onto the magnetosphere rises and, correspondingly, the magnetosphere size is reduced) the star becomes the accretor. However it is not specified how matter is ejected from the accretor. For instance, in the well–known polars, where gas is accreted onto the surface of the white dwarf, no powerful, all the more jet–like outflow of matter is observed. As we have seen, the gas accretion rate in MWC 560 is much lower than the critical, moreover, neither luminosity nor gas accretion rate onto the magnetosphere changes consider-

ably in different states of this object. We have found above that in different activity states of the object only the gas ejection velocity changes essentially. Besides, in the active state the gas velocity is strongly variable, accordingly the brightness variability amplitude increases. What is more, in the active state the luminosity of the UV source is two times higher. To achieve the observed luminosity of MWC 560 the required rate of accretion onto the surface of the white dwarf of radius $5 \cdot 10^8$ cm and mass $1\,M_\odot$ equals $\dot{M}_a = L\,R_{WD}/GM \approx 1.2 \cdot 10^{-6}\ M_\odot/yr$ in the active state and $\approx 6 \cdot 10^{-7}\ M_\odot/yr$ in the passive. When matter is propelled outwards from the magnetosphere, part of it may reach the white dwarf's surface, thus ensuring the observed luminosity. We suppose that the white dwarf in MWC 560 is always under the propeller condition. We interprete the different activity levels of the object as different propeller regimes: the active state of MWC 560 corresponds to the hard propeller, while the passive one to its soft regime. We will discuss this model in more detail below, but first refine the parameters of the hot component, the jet and the system MWC 560.

5. Parameters of the hot component and the jet

It is highly probable that the UV radiation source around the white dwarf of MWC 560 is the photosphere of the powerful wind outflowing from the internal regions. Let us discuss observational evidence for the existence of this wind. The optical and UV spectrum is well described by blackbody radiation from a spherical object with a temperature of ≈ 20000 K and a radius of $\approx 4 \cdot 10^{11}$ cm (Table 2). Along with the detached high-velocity variable absorption lines the low-velocity hydrogen absorption lines are always present (irrespective of the state of the object (Tomov and Kolev, 1997)), which make the line profile of the type P Cyg. The velocity of outflow of gas in which these lines are formed is practically constant and is ≈ -200 km/s for the high members of the Balmer series (Tomov and Kolev, 1997). The depth of these lines is varied: in the passive periods (for example, early 1991) the high-velocity absorptions are getting closer and merge with the low-velocity absorptions, the total absorption line intensity increases. The low-velocity absorption lines may well be formed in the quasi-spherical wind being discussed. The width of the narrow metallic emission lines as well as the emission components of the high Balmer members is FWHM ≈ 100 km/s (Tomov and Kolev, 1997). These lines are probably emitted just above the photosphere of the wind, the metallic lines are formed due to fluorescence of UV radiation (Shore et al., 1994).

For the wind to be formed with the parameters — the luminosity of the photosphere $2 \cdot 10^{37}$ erg/s, the temperature 20000 K and the size $4 \cdot 10^{11}$ cm, and the outflow velocity in the wind $V_w = 100$ km/s — the required rate of the matter outflow is:

$$\dot{M}_W \approx \frac{4\,\pi\,V_w\,R_{out}}{k} \approx 2.0 \cdot 10^{-6} M_\odot, \qquad (1)$$

where $k \approx 0.4$ cm^2/g is the Rosseland absorption cross section (Roger and Iglesias, 1992), which for the approximate parameters of the photosphere, T = 20000 K and $\rho = 4 \cdot 10^{-12}$ g/cm^3 is, in fact, equal to the Thomson cross-section. The density adopted here corresponds to the gas density at the distance R_{out} in the wind outflowing at the rate $\dot{M}_W$ and the velocity V_w. Find the mass loss rate in the jet and kinetic luminosity of the jet (the rate of the kinetic energy flux):

$$\dot{M}_j \approx \pi\,m_p\,\sin^2\theta_j\,N_H\,R_{out}\,V_j \approx 5 \cdot 10^{-7}\,M_\odot/yr, \qquad (2)$$

$$L_k = \dot{M}_j\,V_j^2/2 \approx 6 \cdot 10^{35}\ erg/s. \qquad (3)$$

Here we have used the MWC 560 parameters in the passive state (Table 2, bb2 model): the column density in the jet $N_H = 6 \cdot 10^{23}$ cm^{-2}, the distance from the centre of acceleration to the jet base is assumed equal to the photosphere radius $R_{out} = 4 \cdot 10^{11}$ cm, the velocity of gas in the jet $V_j = 2000$ km/s (Table 1), and the semiopening of the jet $\theta = 20°$. For the active state of the object (model bb1) $\dot{M}_j$ turns out to be the same as for the passive state. As we have noted above, the mass loss rate in the jet as well as the size and temperature of the photosphere of the hot component appear to be constant (within the accuracy of the obtained model parameters) and do not depend on the state of activity of the object. We consider this fact to be of importance and it must be taken into account when selecting a model of the object and discussing the gas acceleration mechanism. One of the most important parameters, which characterizes the efficiency of the jet acceleration mechanism is the ratio of kinetic luminosity of the jets L_k to bolometric luminosity of their source. In the case of MWC 560 the $L_k/L_{bol} \approx 0.05$–0.1 depending on the activity state of the object. If the gas outflow from the object was spherically symmetric, the kinetic luminosity would then be close to the bolometric, which would be difficult to coordinate in the frames of thermodynamics in any model of gas

acceleration. This attests independently the jet–like outflow of gas in MWC 560.

With the matter accretion onto the magnetosphere under the propeller regime part of material may reach the star's surface. This is possible because of the instabilities in plasma — magnetic field interaction, because part of matter falls in the regions close to the axis of rotation, etc. As we have seen above, for the bolometric luminosity of MWC 560 to be provided, depending on the state of the object, $\dot{M}_a \approx (0.6 \div 1.2) \cdot 10^{-6}\ M_\odot/yr$ must be accreted onto the surface of the white dwarf. Obviously, this is the upper limit of the rate of accretion onto the surface since part of radiation (possibly, considerable) is produced through heating and acceleration of gas by the propeller $L_{pr} = L_k/\eta$, where η is the efficiency of the propeller mechanism. We can not estimate the value of η, most likely $\eta < 0.1$. Even in this case (see (3)) the propeller heating furnishes more than 30 % of the UV source luminosity. Thus, the total maximal rate of the gas flow onto the MWC 560 white dwarf makes $\dot{M} = \dot{M}_w + 2\dot{M}_j + \dot{M}_a \approx (3 \div 4) \cdot 10^{-6}\ M_\odot/yr$, or $\approx 3 \cdot 10^{-6}\ M_\odot/yr$ if the luminosity of the object is provided by the propeller only. The main share of the mass (about 50–70 %) outflows at a small velocity (100–200 km/s), forming the optically thick wind, the source of UV radiation of MWC 560, $\lesssim 15$ % of the total mass flow reaches the surface of the white dwarf and approximately 20–30 % is ejected as jets. We have obtained these values from observations, they are rather rough, and some of them are model–dependent.

6. The propeller in MWC 560

The presented gas stream pattern agrees fairly with the present–day knowledge of the propeller mechanism operation at gas accretion onto a rotating magnetic star (see the review of the problem in Lipunov (1987)). This mechanism is very important for the study of gas accretion onto fast–rotating neutron stars. This mechanism is also effective in accretion of interstellar gas onto main sequence magnetic stars (Fabrika and Bychkov, 1988). Now we have to discuss the MWC 560 binary system, i. e. a possibility of accretion of the required mass from the wind of the red giant, the parameters of the white dwarf and its evolutionary status, and also possible mechanisms of collimation of the jets and causes of the different states of the object MWC 560.

To satisfy the observed propeller luminosity and the rate of mass ejection, the second star must lose not less than $\dot{M} \approx 3 \cdot 10^{-6}\ M_\odot/yr$. The average red giant mass loss rate in symbiotic variables is $\approx 10^{-(6 \div 8)}\ M_\odot/yr$ (Mürset et al., 1991), but, probably, even higher in active states. The separation between the components of MWC 560 is $a = \left(\frac{P_{orb}^2}{4\pi^2} G(M_G + M_{WD})\right)^{1/3} \approx 5.7 \cdot 10^{13}$ cm, where, as previously, we take $M_{WD} = 1\ M_\odot$, the orbital period of the system $P_{orb} = 1930^d$, and also the red giant mass $M_G = 1\ M_\odot$, that is the mean value for the symbiotic stars of S type (Whitelock and Munari, 1992). In long–period binaries the orbit is normally elliptical (Boffin et al., 1993). The probable eccentricity value for the MWC 560 orbital period may be estimated as $e = 0.15\,(\log P_{orb} - 1) = 0.34$ (Boffin et al., 1993). Then the minimal distance between the components in MWC 560 may be about $a_p = a(1 - e) \approx 3.7 \cdot 10^{13}$cm. Using this value and the expected mass ratio of the components $q = M_G/M_{WD} = 1$, derive the minimal critical radius (Roche lobe) $R_{cr} = a_p(0.38 + 0.2 \log q) \approx 1.4 \cdot 10^{13}$ cm $= 200\ R_\odot$ (Paczinski, 1971). The typical radius of M4–M5 giants is, however, about $100\ R_\odot$ (Lang, 1992), i. e. twice as small as R_{cr}. The atmosphere of a giant star is not stationary, it outflows irrespective of binarity, the secondary star only intensifies the outflow. For this reason, and also taking into account possible uncertainty in the parameters, we can conclude that the giant star in MWC 560 is capable of overflowing its critical Roche lobe when the white dwarf is crossing periastron.

The gravitational radius of material capture by the white dwarf when travelling on the orbit is $R_g = 2\,G\,M_{WD}/(V_{WG}^2 + V_{orb}^2)$. The orbital velocity of the white dwarf, as has been seen above, is $\approx$ 10 km/s, the mean wind velocity of the red giants is $V_G = 10$ km/s (Nugis et al., 1989). At these values of the parameters it is not difficult to find that $R_g \approx a$. This means that irrespective of whether the giant overfills its critical lobe, the white dwarf may capture and accrete nearly all matter being lost by the giant. This inference can be backed up if one pays attention to the fact that the orbital velocity is comparable in value with the velocity of the wind outflow. The main portion of the gas lost can not leave the system, it must be captured by the white dwarf. From this, in particular, the important conclusion follows that the rate of the gas accretion onto the white dwarf may not be strongly varied with orbital phase. The same conclusion has been drawn above, based on modelling the continuous spectrum of MWC 560. It is possible that in a system having such parameters

the accretion regime (disk or spherical) may alternate depending on the orbital phase. For instance, at periastron the giant may overfill its critical Roche lobe — an accretion disk is formed, in the opposite point of the orbit a white dwarf "gathers" gas of the slow wind — spherical accretion may be possible. To be precise, depending on the phase of the orbit, the specific angular momentum of matter captured by the white dwarf changes. So the pressure of gas falling onto the magnetosphere also changes, which may cause alternation of the propeller action conditions.

The propeller mechanism of gas ejection by a star's rotating magnetic field has been first suggested for neutron stars by Shvartsman (1970) and has been developed in a number of other works (Illarionov and Sunyaev, 1975; Shakura, 1975; Halloway et al., 1978; Wang, 1979; Davies et al., 1979, Davies and Pringle, 1981) (see Lipunov, 1987). Despite the vast study of this problem no reliable propeller model has been created as yet. The nonlinearity makes the problem difficult to resolve. It is supposed that zones of sectorial gas outflow are formed around the propeller, or nonstationary gas ejection occurs when accretion is replaced by outflow. In some propeller scenarios envelopes or disks may be formed round the magnetosphere. It is evident that the propeller ejects gas and carries away angular momentum of the star, however, to define specifically the picture of accretion and outflow has been impossible so far. For the existence of the propeller the magnetic field rotation velocity at the boundary of the magnetosphere (the magnetosphere size or Alven radius R_A) must exceed the velocity of Keplerian rotation of matter at this radius, or, in other words, $R_A > R_c$, where R_c is the radius of corotation. Of vital importance is the knowledge of the velocity of gas ejection. This is what the propeller efficiency depends on, i. e. the momentum loss rate, the rate of evolution of stars etc. As a rule, two cases are considered: 1) a hard propeller, when gas is ejected by the magnetic field at a velocity of its rotation ($2\pi R_A/P$, where P is the star rotation period) (Shakura, 1975; Halloway et al., 1978; Wang, 1979) and 2) a soft propeller, when the magnetic field heats gas and it outflows at a parabolic velocity ($(2GM/R_A)^{1/2}$) (Illarionov and Sunyaev, 1975; Davies et al., 1979; Davies and Pringle, 1981). The magnetic dipole is believed to approach a sphere through a dynamic pressure of accreted gas, therefore the soft propeller scenario is considered as more preferable. However, Wang and Robertson (1985) have performed numerical simulations of the propeller and shown that because of the Kelvin-Helmholtz instability plasmoids may penetrate into a star magnetic field, i. e. be carried along by it and be ejected at a velocity close to the solid–body rotation velocity. Thus the inclusion of possible instabilities in the propeller scheme allows us to expect that the hard version may also be realized.

We suppose that the white dwarf's magnetosphere in the system MWC 560 undergoes transitions of the type "hard-soft" propeller. It is natural to relate the active state (the high, several thousand km/s and variable velocity of gas ejection) to the hard version, while the passive (the outflow velocity is several hundred km/s) to the soft propeller version. For the "hard-soft" propeller transitions no dramatic reconstruction of the magnetosphere is required as is the case with the accretor-propeller transitions (where even the hysteresis effects are expected (Lipunov, 1987)). It is possible that with variations of the rate of gas accretion onto the magnetosphere or with changing the condition of accretion (disk or spherical), instabilities in the layer where magnetic field and gas interact, are suppressed, which caused a change in the mode of gas ejection.

The size of the magnetosphere is determined by equality of the magnetic pressure $B^2/8\pi$ and the dynamic pressure of gas ρV^2, where V is the free-fall velocity, and $\rho V = \dot{M}/4\pi R^2$. The dipole magnetic moment of the star is $\mu = B_0 R_{WD}^3/2$, where B_0 is the magnetic field strength at the pole. Assuming that $\dot{M} = 3 \cdot 10^{-6} M_\odot/yr$ is accreted onto the white dwarf's magnetosphere, derive the magnetosphere size:

$$R_A = \left(\frac{\mu^4}{8\,G\,M_{WD}\,\dot{M}^2}\right)^{1/7} \approx 1.2 \cdot 10^5\, B_0^{4/7}\ \text{cm}. \quad (4)$$

The corotation radius is determined by the rotation period P of the white dwarf:

$$R_c = \left(\frac{G\,M_{WD}\,P^2}{4\,\pi^2}\right)^{1/3} \approx 1.5 \cdot 10^8\, P^{2/3}\,\text{cm}. \quad (5)$$

From the propeller condition $R_A > R_c$ we can find the relationship $B_0 > 8 \cdot 10^8 (P/1000\,s)^{7/6}$ G. The magnetosphere size is $R_A > 1.5 \cdot 10^{10}$ cm, i. e. the magnetosphere is completely hidden from the observer beneath the photosphere of the outflowing wind ($R_{out} \approx 4 \cdot 10^{11}$ cm). For the propeller mode to be realized in MWC 560, the white dwarf must be strongly magnetized. The rotation period $P \sim 1000$ s corresponds to the typical time of the observed brightness variability (10–20 min). The rotating magnetic field is hidden well under the wind's photosphere, and direct

radiation does not reach the observer (it undergoes multiple scattering and is thermalized). Nevertheless, ejection of gas in the active state of the object may disturb the wind and carry the radiation outward. So the object may be variable with a characteristic time of the order of the rotating period of the white dwarf.

Let us estimate the magnetosphere size in other ways. The lowest observed velocity of gas outflow in the passive state (Table 1) is about 600 km/s. Assuming that in this state the propeller is in the soft mode, that is, the gas outflow velocity is $(2GM/R_A)^{1/2}$, find that $R_A \lesssim 7 \cdot 10^{10}$ cm. The inequality here indicates that, depending on the mass of the gaseous envelope lying on the magnetosphere, the outflow may proceed at a velocity lower than the parabolic one. Take now that in the active state the matter ejection velocity in the jets is about 5000 km/s. If the assumption is made that in this state the propeller operates in the hard mode, i. e. the ejection velocity is close to the solid-body velocity of magnetospheric rotation, find $R_A \approx 8 \cdot 10^{10}(P/1000\,s)$ cm. The closeness of the magnetosphere radius values obtained for the hard and soft modes supports the conclusion that these modes do exist, i. e. the theoretical models of propeller are reliable enough.

Under the assumption that $R_A \lesssim 7 \cdot 10^{10}$ cm, find the pole magnetic field strength of the white dwarf, $B_0 \lesssim 1 \cdot 10^{10}$ G. From the condition $R_A > R_c$ find the white dwarf maximal possible rotation period, $P < 2.8$ hours. The strong magnetic field of the white dwarf in MWC 560 is likely to be the necessary condition of the gas ejection due to the propeller mechanism. The interval of magnetic field pole strengths we have found, $10^9\,G \lesssim B_0 \lesssim 10^{10}$ G, corresponds to the surface magnetic fields of $3 \cdot 10^8\,G \lesssim B_S \lesssim 3 \cdot 10^9$ G. Such magnetic white dwarfs are known (Schmidt et al., 1990) among single objects. The frequency of white dwarfs with such strong magnetic fields (Fabrika and Valyavin, 1997) is about 5 % among the magnetic white dwarfs. The magnetic field strength on white dwarfs among polars (magnetic white dwarf coupled with a dwarf of G–M spectral type) makes $10^6 \div 10^8$ G. For the MWC 560 white dwarf evolution, it is essential that this star is a wide pair with a giant. After completion of the giant stage and formation of the second degenerate star, from the observational viewpoint this magnetic white dwarf will not at all differ (after the young white dwarf gets cooler) from a single star.

In the model discussed, the gas outflow in MWC 560 will proceed until the giant phase is completed or the white dwarf slows down its rotation. Deceleration of magnetic white dwarf is the most effective in the propeller state. The time–scale of deceleration is determined by the force moment that affect the magnetosphere, which equals $2\pi \dot{M}_j R_A^2/P$. The deceleration time is $t_d \approx M_{WD} R_{WD}^2/\dot{M}_j R_A^2$. Assuming that in the most active state (as in the spring of 1990) the object stays, on average, for about 10 % of the total time and taking the above limits to the magnetosphere radius, $1.5 \cdot 10^{10}\,cm \lesssim R_A \lesssim 7 \cdot 10^{10}$ cm, find the deceleration time $t_d \approx 10^3 \div 2 \cdot 10^4$ years. The time–scale of evolution of a giant at this stage is about $M_G/\dot{M} \sim 2 \cdot 10^5$ years. After formation of the white dwarf in MWC 560, it was at the propeller or ejecting stage (Lipunov, 1987). When the secondary star of the system entered the red giant phase, the rate of gas accretion onto the magnetosphere of the white dwarf grew to $\dot{M} \sim 10^{-6}\,M_\odot/yr$, and the white dwarf entered the state being observed presently. Several thousand years after deceleration of rotation of the white dwarf, accretion onto the surface will be permitted, i. e. the star will pass to the accretor stage, at which secondary acceleration of rotation is possible. The final state of the white dwarf rotation in the evolution scenario depends on the state of the giant star. We can say that in any case from MWC 560 a wide pair is formed, which consists of two white dwarfs. One of them (magnetic) will rotate with a period from 10–20 minutes to several hours.

The propeller model in MWC 560 allows both the nature of the hot component of the system and its sporadic variability (flickering), and the origin of the jets to be explained. From observations of MWC 560 we know that jet–like outflow of matter occurs in the direction perpendicular to the accretion disk (in any case it is along the angular momentum of the accreting matter). The opening of the jets is sufficiently large, $2\theta_j \gtrsim 40°$. So a more suitable term for the MWC 560 jets would be the anisotropic wind or the sectorial structure of matter outflow described by Shakura (1975). One of the promising models appropriate for the propeller is the collimation of jets with the aid of magnetic field (see references in Livio, 1996). Blanford and Payne (1982) have considered the picture of acceleration and collimation of gas by magnetic field above the accretion disk. This picture may be suited to the case of collimation of gas ejected by the propeller. Gas is entrapped by the magnetosphere magnetic field, in so doing the field is distorted, the open magnetic lines form a toroidal field component. Above the magnetosphere the toroidal field gets pre-

dominant and may accelerate and collimate gas along the axis of rotation. It does not seem possible to give a more specific description of the picture of acceleration and collimation of gas in MWC560. The bulk of observational evidence permits one to hope that the object will stimulate the further development of the propeller model.

7. Conclusions

Spectroscopy results obtained at the 6 m telescope for the unusual symbiotic star MWC560 in the period from the autumn of 1990 to the spring of 1993 are presented. The high-velocity absorption lines of H I, $D_1 D_2$ Na I, Fe II(42) and He I, whose radial velocity varies on a time–scale of several months and is equal to $-500 \div -2500$ km/s, are permanently present in the spectrum. The shape of the high–velocity absorption profiles in the spectrum of MWC560 suggests that these are formed in a jet directed towards the observer. These absorption lines are variable at times shorter than one day with an amplitude of about 10 %. A fast variability for a time of $\lesssim 3$ hours has been detected. Evidence has been found for the existence of an opposite jet directed away from the observer: in the red wing of the Hα line there is extra and variable radiation, whose radial velocity corresponds to the velocity of matter ejection in the jets measured from the absorption lines.

From the constancy of emission line radial velocities the inclination angle $i \approx 10°$ has been estimated. The continuous spectrum has been modeled from the UV to IR range in two different, active and passive, states of the object. The observed spectrum is formed by a star of spectral class M4–5 III, a hot source and an absorbing screen (the jet). The most likely spectral class of the giant star is M4. The interstellar extinction to MWC560 is $A_V \approx 1^m.4$, the extinction to the giant star may be by $0^m.2$ greater. Parameters of the MWC560 jets and physical conditions of gas in them have been estimated. The opening of the jet is $2\theta_j \gtrsim 40°$, its length at the place where the absorbent is located is $\approx 1 \cdot 10^{12}$ cm. The temperature and the density of gas in the jet are $T_j \approx 8000$ K and $n \approx 5 \cdot 10^{11}$ cm^{-3}. The density on the line of sight is varied, $N_H \approx (3 \div 6) \cdot 10^{23}$ cm^{-2}. In different activity states of the object only the velocity of gas ejection (and accordingly the value of N_H) changes at an approximately constant mass loss rate in the jet, $\dot{M}_j \approx 5 \cdot 10^{-7} M_\odot$/yr. The luminosity of the object $L_{bol} \approx 2 \cdot 10^{37}$ erg/s is mainly due to the UV source with the temperature $T \approx 20000$ K, whose radius is $R \approx 4 \cdot 10^{11}$ cm. The hot source is, apparently, the photosphere of strong wind ($\dot{M}_j \approx 2 \cdot 10^{-6} M_\odot$/yr) outflowing from the region around the white dwarf at a velocity of 100 – 200 km/s.

We suppose that the wind and the jets are accelerated in the magnetic field of the white dwarf which accretes gas from the wind of the giant under the propeller regime. The gas is supplied through the accretion disk and ejected by the rotating magnetic field. A sectorial structure of the gas outflow (the jet) is formed. The different activity states of the object may correspond to different modes: a hard propeller with a gas ejection velocity of several thousand km/s and soft propeller with an ejection velocity of hundreds of km/s. The total rate of gas accretion onto the propeller is $\dot{M} = 3 \div 4 \cdot 10^{-6} M_\odot$/yr. The greater part of this matter (about 50–70 %) outflows as a slow wind. Not more than 15 % of gas accreted onto the magnetosphere may reach the surface of the white dwarf. This share depends on which proportion of the object's luminosity (may be the whole luminosity) can be provided by the propeller. About 20–30 % of the initial captured mass is ejected as jets.

For the effective operation of the propeller, the white dwarf in MWC560 must be strongly magnetized. The strength of its surface magnetic field may be $3 \cdot 10^8$ G $\lesssim B_S \lesssim 3 \cdot 10^9$ G, the period of its rotation may lie within the interval from 10–20 minutes to 3 hours. The lower limit of the period is close to the scale of photometric flickering of the object, therefore the period of its rotation is likely to be about 10–20 minutes. The magnetic field strength on the magnetosphere may amount to $\sim 10^4$ G. The magnetosphere is completely hidden from the observer under the photosphere of the slow outflowing wind. Direct observations of radiation from the magnetosphere or from the surface layers are impossible since it is scattered much once before it appeares on the photosphere. It is possible that in active periods, when gas is ejected in portions at a velocity of several thousand km/s, channels may be formed in the gas envelope through which the observer can recognize bursts of hard or polarized radiation. Further spectral and photometric observations of MWC560 are of great importance.

Acknowledgements. The authors are grateful to D. Kolev, E. L. Chentsov and S. Popov for helpful discussions, A. I. Shapovalova and A. N. Below for assistance in observations, S. Sergeyev and G. Galazutdinov for programmes for reduction of spectra. A.A.P. thanks the Bulgarian National Astronomical Observatory "Rozhen" for welcome during the work over the paper. The work has

been supported by the RFBR through grant 96-02-16396. Thanks of T.T. are due to the Bulgarian Foundation of Scientific Researches for support by grant F-35/1991.

References

Blanford R.D., Payne D.C., 1982, Mon. Not. R. Astron. Soc., **199**, 883

Boffin H.M.J., Cerf N., Paulus G., 1993, Astron. Astrophys., **271**, 125

Cardelli J.A., Clayton G.C., Mathis J.S., 1989, Astrophys. J., **345**, 245

Castor J.I., Lamers H.J.G.L., 1979, Astrophys. J. Suppl. Ser., **39**, 481

Davies R.E., Fabian A.C., Pringle J.E., 1979, Mon. Not. R. Astron. Soc., **186**, 779

Davies R.E., Pringle J.E., 1981, Mon. Not. R. Astron. Soc., **196**, 209

Doroshenko V.T., Goranskij V.P., Efimov Y.S., 1993, Inf. Bull. Var. Stars., **3824**

Drabek S.V., Kopylov I.M., Somov N.N., Somova T.A., 1986, Bull. Spec. Astrophys. Obs., **22**, 64

Fabrika S.N., Bychkov V.D., 1988, in: Glagolevsky Yu.V. and Kopylov I.M. (eds), "Magnetic Stars", Leningrad, "Nauka", 241

Fabrika S.N., Dressel H., Hassal B., 1991 (unpublished).

Fabrika S.N., Valyavin G.G., 1997, in: Glagolevskij Yu.V., Romanuyk I.I. (eds), "Stellar Magnetic Fields", Moscow, "Nauka", 132

Gazhur E.B., Klochkova V.G., Panchuk V.E., 1990, Pis'ma Astron. Zh., **16**, 473

Greenstein J.L., Oke J.B., 1982, Astrophys. J., **258**, 209

Halloway N., Kundt W., Wang Y.-M., 1978, Astron. Astrophys., **70**, L23

Illarionov I.F., Sunyaev R.A., 1975, Astron. Astrophys., **39**, 185

Lang K.R., 1992, Astrophysical Data. Berlin, Planet and Stars: New York

Lipunov V.M., 1987, Astrophysics of neutron stars, Moscow: "Nauka"

Livio M., 1996, Prepr. STSI **1097**

Lynden-Bell D., Pringle J.E., 1974, Mon. Not. R. Astron. Soc., **168**, 603

Maran S.P., Michalitsianos A.G., Oliversen R.J., Sonneborn G., 1991, Nature, **350**, 404

Michalitsianos A.G., Maran S.P., Oliversen R.J., Bopp B., Kontizas E., Dapergolas A., Kontizas M., 1991, Astrophys. J., **371**, 761

Mürset U., Nussbaumer H., Schmidt H.M., Vogel M., 1991, Astron. Astrophys., **248**, 458

Nugis T., 1989, Mass Loss from Stars: the Universal Formula for Mass Loss Rate, ENSV TA, Tallin

O'Donnell J.E., 1994, Astrophys. J., **422**, 158

Paczynski B., 1971, Annu. Rev. Astron. Astrophys., **9**, 183

Paczynski B., Zytkov A.N., 1978, Astrophys. J., **222**, 604

Ritter H., 1991, Astrophys. J., **376**, 177

Robinson E.L., 1976, Annu. Rev. Astron. Astrophys., **14**, 119

Rogers F.J., Iglesias C.A., 1992, Astrophys. J. Suppl. Ser., **79**, 507

Schmidt G.D., Latter W.D., Foltz C.B., 1990, Astrophys. J., **350**, 758

Shakura N.I., 1975, Pis'ma Astron. Zh., **11**, 23

Shakura N.I., Sunyaev R.A., 1973, Astron. Astrophys., **24**, 337

Shore S.N., Aufdenberg J.P., Michalitsianos A.G., 1994, Astron. J., **108** 671

Shvartsman V.F., 1970, Radiofisika, **13**, 1852

Taylor A.R., Seaquist E.R., Mattei J.A., 1986, Nature, **319**, 38

Thakar A., Wing R.F., 1992, Bull. Amer. Astron. Soc., **24**, 801

Tomov T., Kolev D., Georgiev L., Zamanov R., Antov A., Bellas Y., 1990, Nature, **346**, 637

Tomov T., Zamanov R., Kolev D., Georgiev L., Antov A., Mikolajewski M., Esipov V., 1992, Mon. Not. R. Astron. Soc., **258**, 23

Tomov T., Kolev D., Michalitsianos A.G., Mikolajewski M., Sonneborn S.N., Maran S.P., Oliversen R.J., Sonneborn G., 1994, Prepr. of Institute of Astronomy Nicolaus Copernicus University, **33**

Tomov T., Kolev D., Ivanov M., Antov A., Jones A., Mikolaewski M., Leperdo A., Passuello R., Saccavino S., Sostero G., Valentinuzzi T., Bellas-Vellidis Y., Dapergolas A., Murani U., 1996, Astron. Astrophys. Suppl. Ser., **116**, 1

Tomov T., Kolev D., 1997, Astron. Astrophys. Suppl. Ser., **122**, 43

Wang Y.-M., 1979, Astron. Astrophys., **74**, 253

Wang Y.-M., Robertson J.A., 1985, Astron. Astrophys., **151**, 361

Whitelock P.A., Munari U., 1992, Astron. Astrophys., **255**, 171

Zhekov S.A., Hunt L.K., Tomov T., Gennari S., 1996, Astron. Astrophys., **309**, 800